Supporting Information

Pressurized well-inspired triboelectric nanogenerators for harvesting water wave energy toward marine environmental applications

Yan Wu[a,b,c], Xiutong Wang[a,c,d]*, Lihui Yang[a], Youqiang Wang[c], Youbo Nan[a,b,d], Hui Xu[a], Hui Zhou[a], Weilong Liu[a]

[a] State Key Laboratory of Advanced Marine Materials, Key Laboratory of Marine Environmental Corrosion and Bio-fouling, Institute of Oceanology, Chinese Academy of Sciences, Qingdao 266071, China

[b] Institute of Marine Corrosion Protection, Guangxi Key Laboratory of Marine Environmental Science, Guangxi Academy of Sciences, Nanning 530007, China

[c] Qingdao University of Technology, Qingdao 266525, China

[d] University of Chinese Academy of Sciences, Beijing 100049, China

* Corresponding author: wangxiutong@qdio.ac.cn

ORCID iD: https://orcid.org/0000-0001-8389-2080

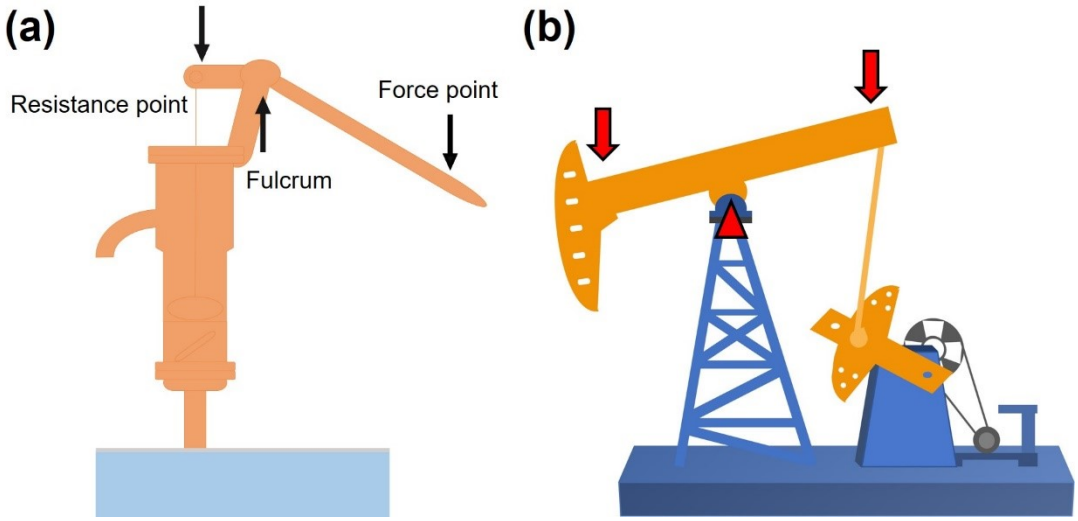

Figure S1. Schematic of (a) pressure well and (b) beam pumping unit.

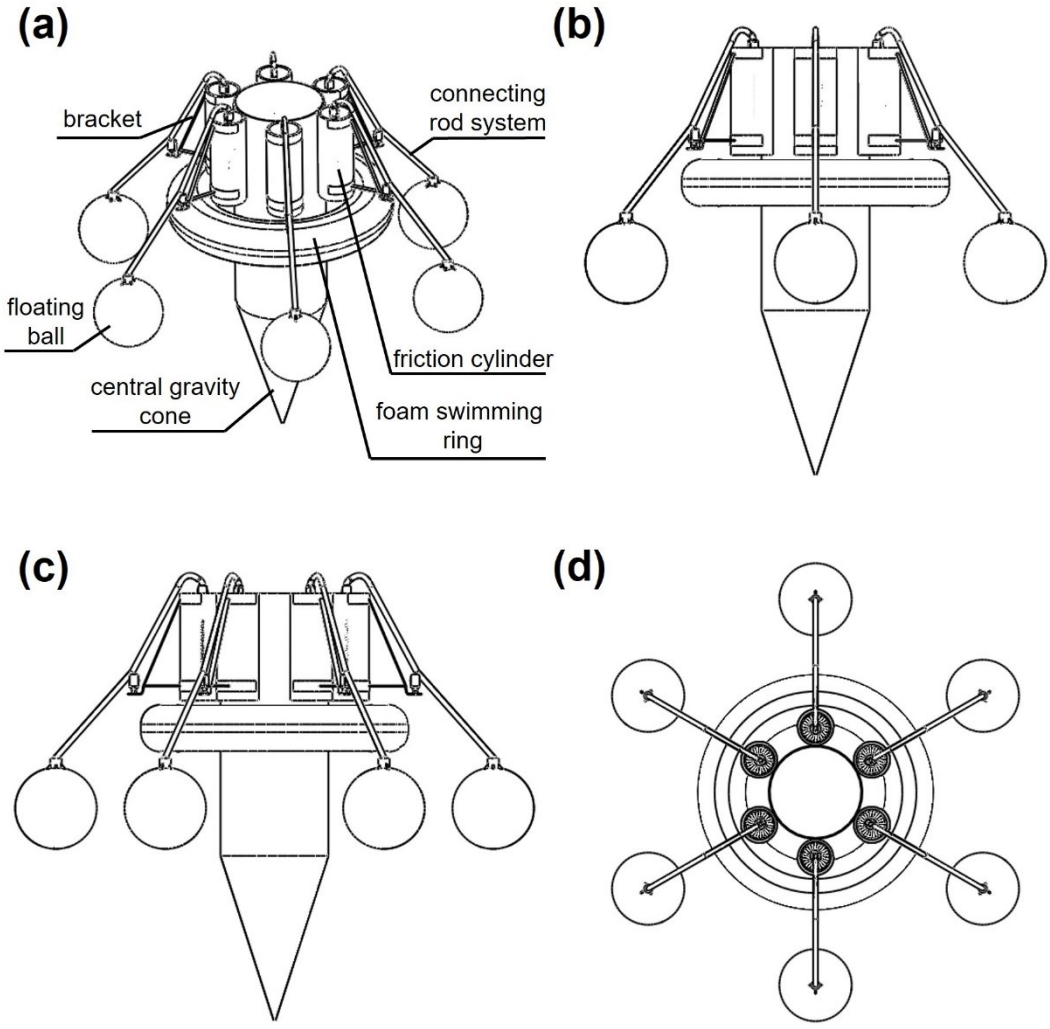

Figure S2. (a) Stereogram (b) right view (c) front view (d) top view of IPW-TENG.

Figure S3. Digital photographs of foam swimming ring.

Figure S4. Digital photographs of floating ball.

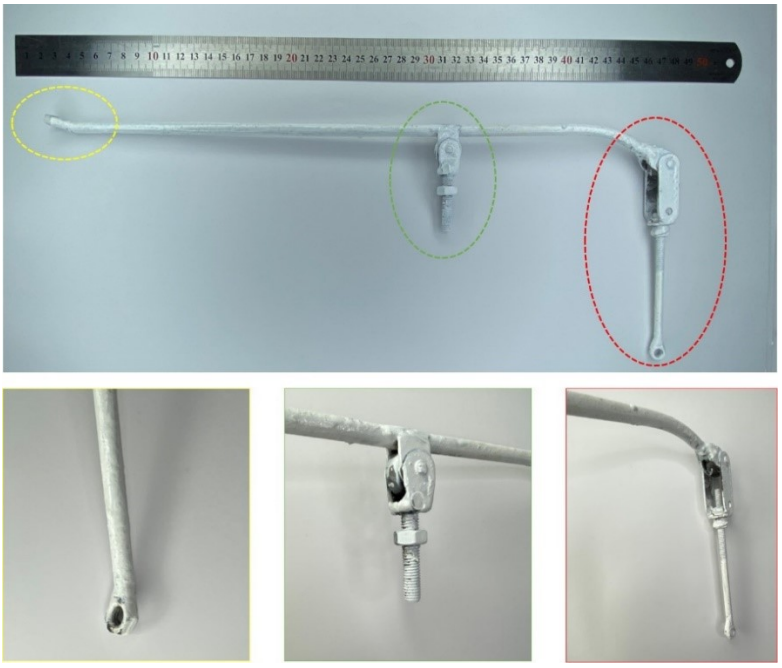

Figure S5. Digital photographs of connecting rod system.

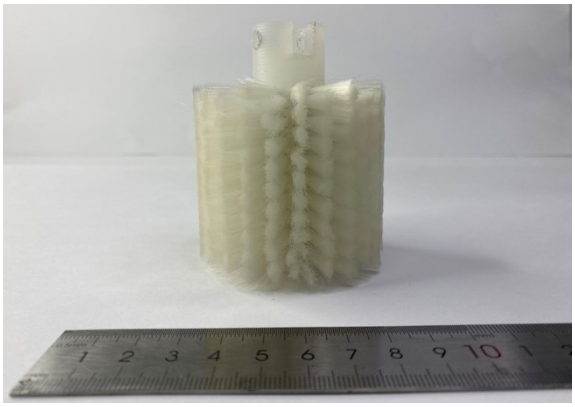

Figure S6. Digital photographs of nylon brush.

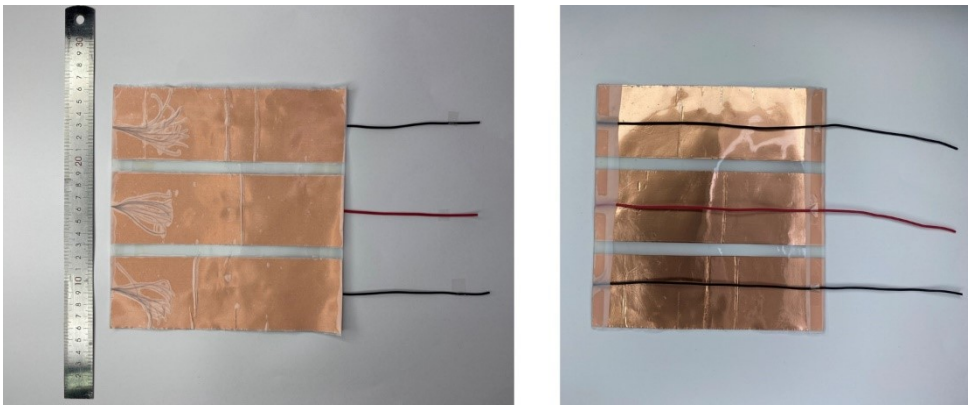

Figure S7. Digital photographs of PTFE film and copper electrode attached to PET film.

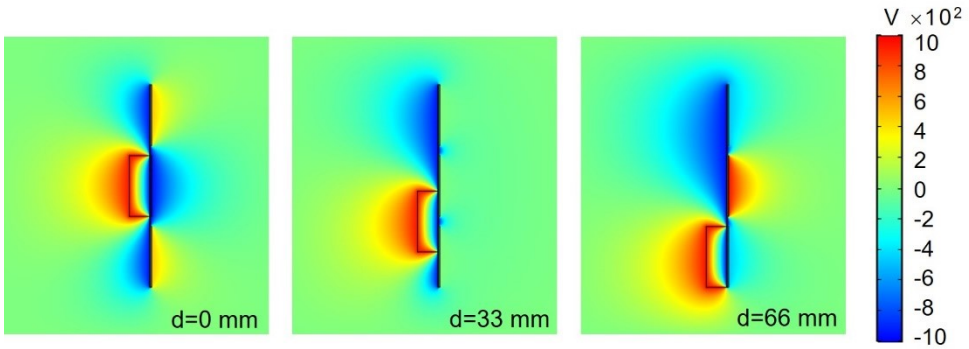

Figure S8. Finite element simulations of qualitative potential distributions for various positions of the IPW-TENG of single power generation unit.

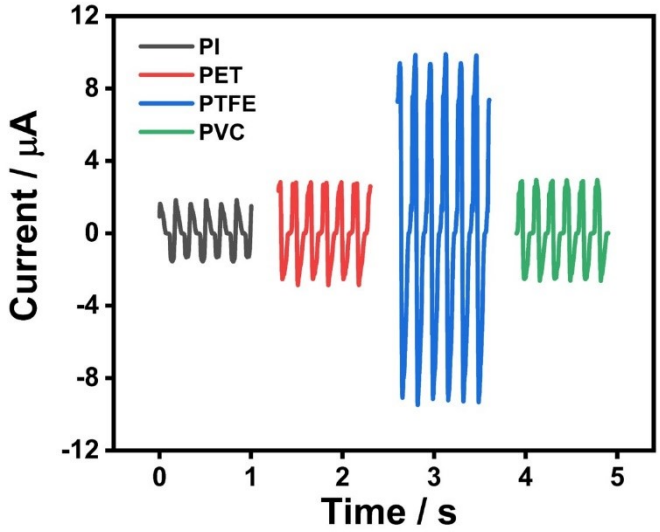

Figure S9. Short circuit current of IPW-TENG under different negative friction materials.

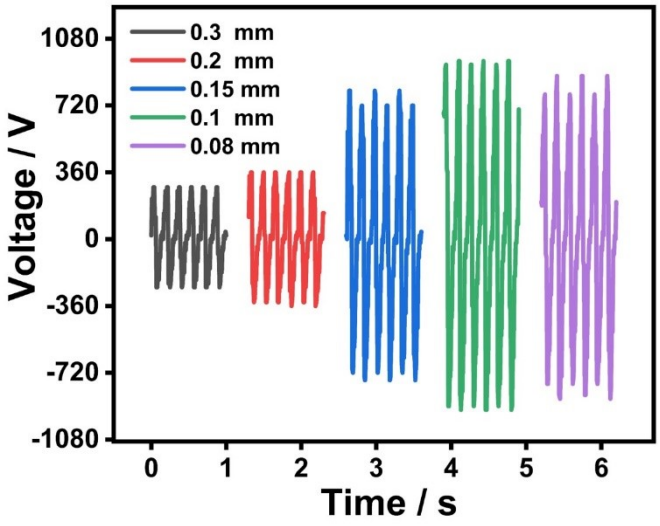

Figure S10. Open circuit voltage of IPW-TENG with different bristle diameters.

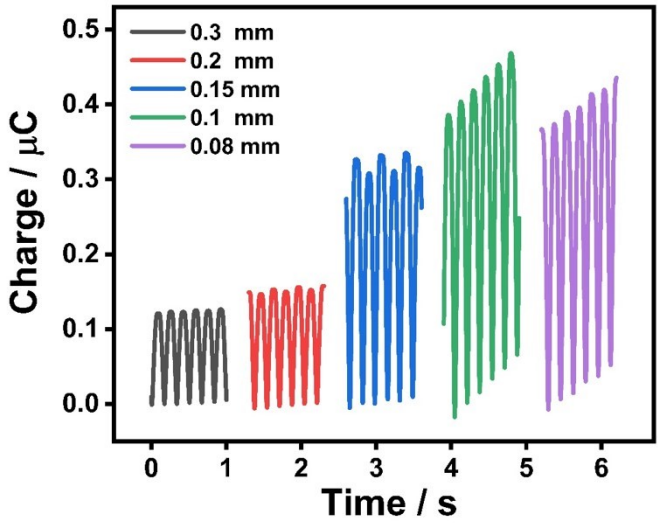

Figure S11. Transferred charge of IPW-TENG with different bristle diameters.

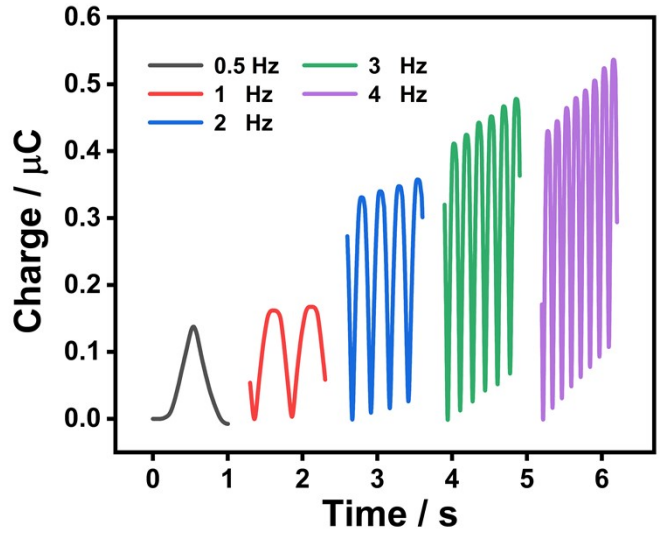

Figure S12. Transferred charge of IPW-TENG with different frequency.

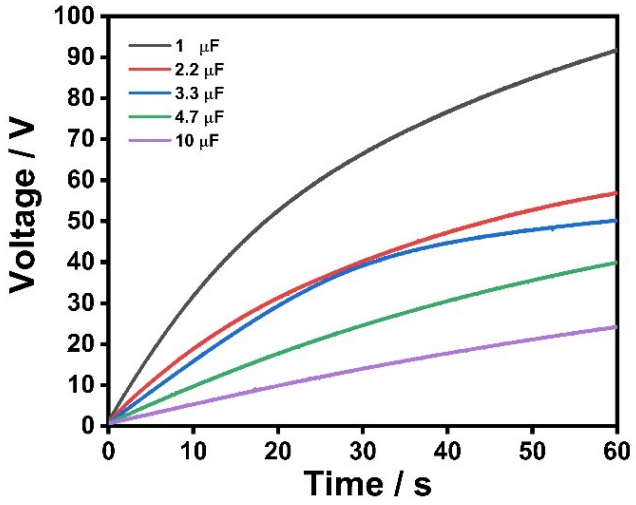

Figure S13. Charging curve of IPW-TENG to capacitors of different capacities.

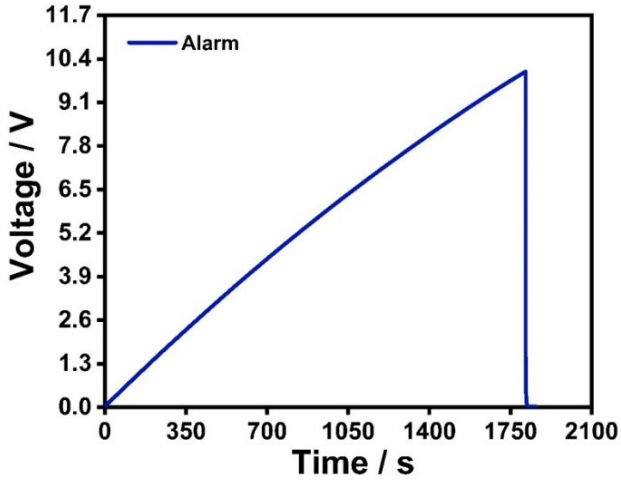

Figure S14. Charging curve of IPW-TENG to alarm.

Table S1. Candidate materials for triboelectric layers.

Triboelectric layer materials
Polydimethylsiloxane (PDMS)
Polypropylene (PP)
Polyethylene (PE)
Polystyrene (PS)
Polyvinylidene Chloride (PVDC)
Polyacrylonitrile (PAN)
Modacrylic (Modacrylic Fiber)
Polyisobutylene (PIB)

Table S2. Comparison between IPW-TENG and the predecessors.

Device	Voltage (V)	Current (μA)	Power (mW)	Refs.
CEP-TENG	90	0.24	0.0054	1
RS-TENG	1400	0.8	0.62	2
MFA-TENG	250	18	0.68	3
GA-TENG	240	4	3	4
IPW-TENG	960	9.8	3.124	This work

Table S3. Experimental conditions for the electrochemical impedance.

A.C. impedance parameters		
Init E (V)	-0.4	
High Frequency (Hz)	100000	
Low Frequency (Hz)	0.01	
Amplitude (V)	0.01	
Quiet Time (sec)	2	
Sensitivity Scale Setting	Automatic	
Measurement Mode above 100 Hz	Single Freq.	
Measuring Time or Cycles and Points	Avrg/Cycles	Points / Decade Freg
	1	12
Bias DC Current During Run	Below 1 Hz	

Reference:

1. R. Ouyang, J. Miao, T. Wu, J. Chen, C. Sun, J. Chu, D. Chen, X. Li and H. Xue, *Adv. Mater. Technol.*, 2022, **7**, 2200403.
2. F. Huang, P. Yang, Z. Liu, D. Yang, L. Huang, Y. Shi, X. Tao, Y. Chen, H. Li, X. Chen and Z. Bian, *Nano Energy*, 2023, **110**, 108346.
3. M. Ding, J. Wang, D. Zhao, H. Li, X. Cheng, J. Wen, Z. L. Wang and T. Cheng, *Nano Research*, 2024, **17**, 7144-7152.
4. Q. Gao, J. Wang, H. Li, Y. Yu, X. Zhang, Y. Wang, J. Wen, Z. L. Wang and T. Cheng, *Chem. Eng. J.*, 2024, **493**, 152730.